

Bayesian Neural Networks for Fast SUSY Predictions

B. S. Kronheim^a, M. P. Kuchera^a, H. B. Prosper^b, A. Karbo^a

^a*Department of Physics, Davidson College, NC, USA*

^b*Department of Physics, Florida State University, FL, USA*

Abstract

One of the goals of current particle physics research is to obtain evidence for new physics, that is, physics beyond the Standard Model (BSM), at accelerators such as the Large Hadron Collider (LHC) at CERN. The searches for new physics are often guided by BSM theories that depend on many unknown parameters, which, in some cases, makes testing their predictions difficult. In this paper, machine learning is used to model the mapping from the parameter space of the phenomenological Minimal Supersymmetric Standard Model (pMSSM), a BSM theory with 19 free parameters, to some of its predictions. Bayesian neural networks are used to predict cross sections for arbitrary pMSSM parameter points, the mass of the associated lightest neutral Higgs boson, and the theoretical viability of the parameter points. All three quantities are modeled with average percent errors of 3.34% or less and in a time significantly shorter than is possible with the supersymmetry codes from which the results are derived. These results are a further demonstration of the potential for machine learning to model accurately the mapping from the high dimensional spaces of BSM theories to their predictions.

Keywords: SUSY, neural networks, Bayesian, machine learning

1. Introduction

The discovery of the Higgs boson at the LHC in 2012 [1, 2] marked the end of the search for the Standard Model (SM) particles. With the completion of the SM, physicists' focus over the next decade or so is understanding the physics of electroweak symmetry breaking [3] by following two broad strategies: comparing precision measurements of Higgs boson properties with SM predictions [4] and conducting direct searches for physics beyond the SM. This marks a methodological change in particle physics, moving from a well-posed search for particles predicted by a well-tested theory, to searching for any evidence of new physics guided, in part, by the predictions of BSM theories. A popular group of candidate theories for beyond the SM physics are the supersymmetric (SUSY) theories. These theories provide potential solutions to the hierarchy problem, permit gauge cou-

pling unification at high energies [5], and provide a promising candidate for a dark matter particle [6].

The simplest formulation of supersymmetry consistent with the Standard Model is the Minimal Supersymmetric Standard Model (MSSM). The MSSM uses the same gauge group as the Standard Model and assumes minimal particle content and R-parity conservation. Despite being a minimal model, the MSSM has 105 free parameters [7] beyond those of the SM, making a thorough exploration of the model challenging. The typical approach is to select a set of parameter points within an accessible subset of the parameter space and compute observables, such as cross sections, for each point. While meaningful results have been obtained from approaches like this [8], the expensive computations limit our ability to investigate the theoretical parameter spaces thoroughly and limit our ability to use standard likelihood methods [9] to make inferences about the parameter spaces. Through the methods outlined in this paper we show that an accurate, fast, mapping of BSM theory parameters to predictions can be constructed based on recently available tools that implement

Email addresses: brkronheim@davidson.edu (B. S. Kronheim), mikuchera@davidson.edu (M. P. Kuchera), akarbo@fsu.edu (A. Karbo)

sampling via Hamiltonian Monte Carlo (HMC).

A simplification of the full MSSM, which is also a prototypical example of a BSM theory that is currently under intense theoretical and experimental investigation, is the phenomenological MSSM (pMSSM) [10, 11, 12, 13, 14]. The pMSSM has no new sources of CP-violation, no flavor changing neutral currents, and includes first and second generation universality. These assumptions, which are consistent with experimental facts, reduce the 105 free parameters to just 19 [14]. The large reduction in the number of free parameters is useful in that it renders calculations with this model feasible, while being large enough to make the pMSSM a good proxy of the MSSM. The parameter space is also complex enough to highlight the advantages of the use of machine learning for the rapid calculation of observables. While this is the theory studied in this paper, the pMSSM is merely an interesting example of a high-dimensional theory that illustrates the technique discussed in this paper.

Machine learning has been successfully applied to several problems in high energy physics [15] and SUSY in particular. In Ref. [16], neural networks were shown to be capable of determining restrictions on parameter values given experimental evidence and in [17] random forests were used to classify pMSSM parameter combinations as excluded or not excluded by ATLAS and CMS searches. Additionally, Bayesian neural networks, the type of machine learning used in this paper, along with boosted decision trees, were used in [18, 19, 20] to aid in the detection of single top quarks at the Tevatron as well as in neutrino background and signal discrimination [21]. For recent reviews of the use of machine learning in the physical sciences see, for example, [15, 22] and the recently released machine learning inference toolkit `MadMiner` [23].

In this paper, we use Bayesian neural networks [24] to model the mapping of the parameter space of the pMSSM to its predictions. The program `SOFTSUSY` [25] is used to calculate particle spectra and decay chains, while the program `Prospino2` is used to calculate cross sections for neutralino chargino pair production [26] at the LHC at 14 TeV [27]. These programs encode algorithms that give accurate predictions, but only point by point in the parameter space. However, given predictions computed at a large number of parameter points, we show how Bayesian neural networks (BNNs) can be used to create prediction functions that map parameters to predictions. This is demon-

strated for three different prediction functions:

1. A map from parameters to a classification of whether a given pMSSM parameter point is physically or numerically viable as determined by `SOFTSUSY`.
2. A map from parameters to the predicted cross section for neutralino chargino production.
3. A map from parameters to the predicted light neutral Higgs boson mass.

With these functions, it is possible to assess quickly whether a pMSSM parameter point is valid, whether it yields a Higgs boson mass consistent with the observed value, and predict the cross section for neutralino chargino production.

2. Mathematical Details

Our goal is to predict the physical or numerical viability of pMSSM parameter points, predict the neutralino chargino production cross section, and predict the mass of the lightest neutral Higgs boson, and to do so as accurately and rapidly as possible. The pMSSM parameters are listed in Table 1. In

Parameter	Description	Range
M_1	bino mass	$ M_1 \leq 4$ TeV
M_2	wino mass	$ M_2 \leq 4$ TeV
M_3	gluino mass	$M_3 \leq 4$ TeV
μ	higgsino mass	$ \mu \leq 4$ TeV
M_A	pseudoscalar Higgs boson mass	$M_A \leq 4$ TeV
$\tan \beta$	ratio of vacuum expectation values of Higgs doublets	$1 \leq \tan \beta \leq 60$
A_t, A_b, A_τ	third generation trilinear coupling	$A \leq 7$ TeV
$m_{\bar{q}}, m_{\bar{u}_R}, m_{\bar{d}_R}, m_{\bar{l}}, m_{\bar{e}_R}$	first/second generation sfermion mass parameters	$m \leq 4$ TeV
$m_{\bar{Q}}, m_{\bar{t}_R}, m_{\bar{b}_R}, m_{\bar{L}}, m_{\bar{\tau}_R}$	third generation sfermion mass parameters	$m \leq 4$ TeV

Table 1: The 19 parameters of the pMSSM and the subset of the pMSSM parameter space considered in this paper.

this paper, we model these functions as Bayesian neural networks (BNN) [24].

2.1. Bayesian neural networks

In the Bayesian approach to neural networks [24], the goal is to infer a probability density $p(\theta | D)$ over the parameter space of the network, Θ , given training data D . A Bayesian neural network is a functional

$$p(x, D) = \int F(x, \theta) p(\theta | D) d\theta \quad (1)$$

of the posterior density

$$p(\theta | D) = \frac{p(D | \theta) \pi(\theta)}{p(D)}, \quad (2)$$

where $p(D | \theta)$ is the likelihood of the data, $\pi(\theta)$ a prior density, and $F(x, \theta)$ a function whose average over the space Θ is desired. For example, setting $F(x, \theta) = \delta(y - f(x, \theta))$, where $f(x, \theta)$ is a neural network, yields the predictive density,

$$p(y | x, D) = \int \delta(y - f(x, \theta)) p(\theta | D) d\theta. \quad (3)$$

The training data $D = \{(t_k, x_k)\}$ comprises the targets t_k associated with the pMSSM parameters points x_k . In practice, the posterior density is represented by an ensemble of neural networks whose parameters are sampled from the posterior density using the Hamiltonian Monte Carlo Method [24, 28]. Since the method approximates Eq. (3), it automatically furnishes an estimate of the uncertainty in the predictions y from some measure of the width of the predictive density.

2.2. Likelihood and Prior

Likelihood. We take the likelihood functions $p(D | \theta)$ to be products over Bernoulli densities for the classifier and normal densities for the regression models with targets derived from the training data. For the classifier, these targets are 1 and 0 for the viable and non-viable pMSSM parameter points, respectively, which we denote as `valid` and `invalid`, respectively. For the regression models, the targets are either the cross sections computed using `Prospino2` or the Higgs boson masses computed using `SOFTSUSY`.

Prior. Choosing a high-dimensional prior for likelihood functions as complex as the ones used here is an extremely challenging problem. Therefore, in this case and in general, the prior is chosen for computational simplicity and its ability to yield satisfactory results. Furthermore, by using a hierarchical prior whose parameters are constrained by

a hyper-prior, increased flexibility is introduced in the choice of prior. The overall prior $\pi(\theta)$ is a product of the priors for all network parameters and the associated hyper-priors. For additional details see [29].

3. Data Sets

In this section, we describe the data sets used to construct the prediction functions, that is, the functions mapping pMSSM parameter points to predictions as well as the metrics used to assess the quality of the function approximations.

The training data for each prediction function consists of points sampled from a bounded subset of the pMSSM parameter space together with the associated predictions. We adopt the pMSSM parameter bounds given in [12] and [30] that limit sparticle masses to those within reach of the LHC. The bounds are reproduced in Table 1. The parameter points are the inputs x_k , while the predictions are the targets t_k .

We use three independent data sets, labeled **VPAR**, **OHIGGS**, **XSEC**, and follow standard practice by dividing each data set into three sets: training, validation, and test sets in the percentages, 80%, 10%, and 10%, respectively. The first set was used to train the BNN models, the second was used to assess the models' performance during training, and the third (the test set) was used to evaluate the performance of the trained models.

VPAR. This data set consists of 500,000 points randomly sampled from the subspace given in Table 1. Each pMSSM parameter is sampled independently from a uniform distribution over its range. For each point, `SOFTSUSY` is used to compute sparticle masses and decays. Of the points sampled, 60.61% were labeled as invalid and 39.39% as valid.

OHIGGS. This data set consists of 567,597 points with sparticle masses computed using `SOFTSUSY`. The points were sampled in the same way as for **VPAR**, but only those points without errors were kept. We additionally only kept those points with a Higgs mass between 110 and 130 GeV, as this contained the majority of the points and had a much smaller range than the full dataset of 591,337 points.

XSEC. This data set consists of 202,264 pMSSM points with decays computed using **SOFTSUSY** and cross sections computed at next to leading order (NLO) accuracy using **Prospino2**. The **SOFTSUSY** calculations were reused from the generation of the **OHIGGS** data set.

3.1. Data preparation

The data sets were prepared for training using several different normalization schemes. For the input parameters, here the 19 pMSSM parameters, we scaled and shifted each parameter to have zero mean and unit variance. The targets of the **VPAR** data set were left unchanged since the values are 0 and 1. The targets of the **XSEC** data set were log normalized, that is, the natural logarithm of the cross sections was computed and the values shifted and scaled to have zero mean and unit variance. This was done because the distribution of the log of the cross section was roughly normal. The **OHIGGS** data set was also normalized to have zero mean and unit variance by subtracting the mean and dividing by the standard deviation.

3.2. Metrics

The ensemble of neural networks $\hat{y} = f(x, \theta_j)$ constitute a point cloud approximation of the predictive distribution $p(y | x, D)$. From the ensemble we can estimate the mean and standard deviation of $p(y | x, D)$, which we take as estimates of the prediction and the uncertainty in the prediction, respectively.

It is important to assess the reliability of the prediction functions by examining the uncertainty estimates, which come with the predictions, as they are the main advantage of BNNs over other machine learning models. The quality of the approximation has been assessed using two main metrics:

- the ratio of the root mean square (RMS), that is, $(E[(\hat{y} - y)^2])^{\frac{1}{2}}$, to the target y and
- the relative frequency with which the the 3-standard deviation interval about the mean of $p(y | x, D)$ brackets the true predictions, y .

The quality of the classifier was assessed using the measures precision, recall, and F_1 [31]. In the current context, the precision is defined by

$$P \equiv P(V | +) = \frac{P(+ | V) N(V)}{P(+ | V) N(V) + P(+ | \bar{V}) N(\bar{V})}, \quad (4)$$

where $R = P(+ | V)$ is the recall and $N(V)$ and $N(\bar{V})$ are the numbers of valid and invalid pMSSM points, respectively. A result is + if a pMSSM point is classified as valid and – otherwise. Note, that the recall can be computed from

$$R \equiv \frac{P(+ | V) N(V)}{P(+ | V) N(V) + P(- | V) N(V)}, \quad (5)$$

where the numerator is the number of true positives and the denominator is the sum of true positives and false negatives. The quantity F_1 is the harmonic mean

$$F_1 = \frac{PR}{(P + R)/2}. \quad (6)$$

Recall is the fraction of valid points that are correctly identified. The quantity F_1 provides a single measure that balances precision and recall. Note that recall is an intrinsic characteristic of a classifier, whereas precision depends on the ratio $N(V)/N(\bar{V})$, which is a property of the data set to which the classifier is applied. In particle physics, the quantity obtained by setting $N(V) = N(\bar{V})$ in the precision, that is, by using a balanced data set, is typically referred to as the discriminant.

In practice, the precision and recall are approximated using the number of true positive predictions, TP , the the number of false positive predictions, FP , and the number of false negative predictions, FN , as follows,

$$P = \frac{TP}{TP + FP}, \quad (7)$$

$$R = \frac{TP}{TP + FN}. \quad (8)$$

For a given input feature vector x , here a pMSSM parameter point, a machine learning model would typically provide a single estimate of the quantity it models, while a BNN model provides a point cloud approximation to the full predictive distribution, Eq.(3). We can assess the impact of using a posterior distribution rather than the output from a single network by noting how the metrics change when applied to the mean, the mean minus 3 standard deviations, and the mean plus 3 standard deviations.

4. Results

For each pMSSM prediction function, and a given pMSSM parameter point x , we use the mean of the

predictive distribution, $p(y|\dot{x}, D)$, as an estimate of the corresponding prediction from either **SOFTSUSY** or **Prospino2**, while the standard deviation of the predictive distribution is taken as an estimate of the uncertainty in the prediction.

4.1. The viability classifier (VPAR)

The three performance metrics for the **VPAR** classifier are given in Table 2. A pMSSM point is classified as valid if the point estimate, the average over the ensemble of networks, exceeds a cutoff of 0.5. Alternatively, one can apply the cutoff to the average plus 3 standard deviations. This causes many points with high uncertainty to be classified as valid and results in a much higher recall score and slightly lower F_1 and precision scores. We expect the average over the ensemble of networks to be most useful for attaining the highest classification accuracy, while the average plus 3 standard deviation would be useful in selecting valid points that could serve as input to a program such as **SOFTSUSY**. The program would catch false positives but not false negatives.

Configuration	Recall	Precision	F_1
Mean	0.955	0.953	0.954
Mean + 3SD	0.982	0.915	0.947

Table 2: **VPAR**: performance metrics.

4.2. The cross section regression function (XSEC)

After training on the **VPAR** data set, networks were trained on the **XSEC** data set. For a given pMSSM parameter point, we again take the average, \hat{y} , of the distribution of network outputs, as an estimate of the quantity being modeled, here the predicted cross section in femtobarns. We use the associated standard deviation, σ , to exclude pMSSM parameter points for which $\log(\hat{y} - 3\sigma) > 3$, as pMSSM points with cross section of this size or larger have been excluded at the LHC [32, 12]. This cut removed 5.5% of the generated pMSSM points. On average, with this cut, the cross section is estimated with a percentage uncertainty of 3.34% and the true value fell within 3 standard deviations of the estimated cross section 99% of the time.

The standard deviation can be used to flag pMSSM points for which the network based prediction is highly uncertain. If we exclude the 45 pMSSM points with cross sections that differ by an

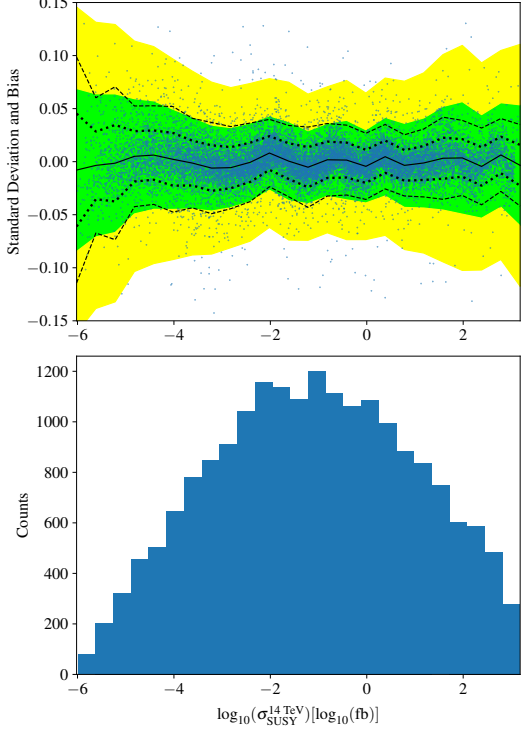


Figure 1: (top) The solid and dotted lines are computed from the errors of the BNN, that is, from the differences between the BNN estimates and the associated true values. The black line is the bias of the BNN as a function of the log of the cross section, while the dotted lines represent the 1 and 2 standard deviation intervals. The green and yellow bands are root mean square intervals computed from the standard deviations furnished by the BNN. (bottom) The distribution of the log cross section.

order of magnitude or more between the bounds $\hat{y} - 3\sigma$ and $\hat{y} + 3\sigma$ the relative uncertainty in the predictions falls to 3.04%.

Figure 1 shows the two measures of uncertainty in the BNN predictions: one computed directly from the known errors of the BNN predictions and the other from the estimated standard deviations of the predictive distribution. The bias in the BNN predictions is negligible. However, the point cloud of network outputs overestimates the uncertainty in the BNN predictions. It is also clear that the BNN behaves as expected in that the uncertainty is greater where there are fewer data for training.

When predicting cross sections for many pMSSM points simultaneously on a GPU, a single prediction per network, in the ensemble of networks, took on average 49 nanoseconds for the prediction alone and 94 nanoseconds when the computational overhead

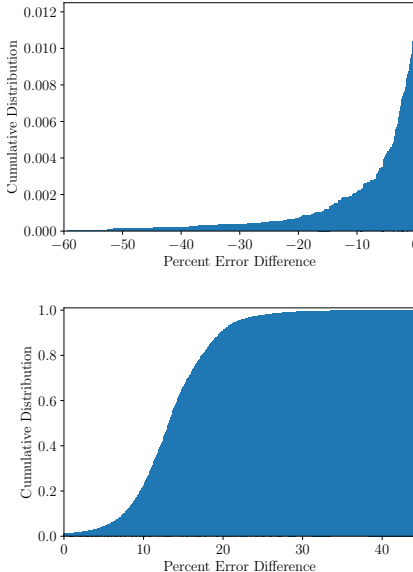


Figure 2: The cdf for the difference in relative uncertainty between (top) the prediction at leading order and that of the BNN and (bottom) between the BNN and the leading order. The vast majority of the BNN-based predictions are more precise, in the sense of being closer to the corresponding NLO predictions, than the predictions at leading order.

is included. The BNN for the above results used 135 networks, which implies a computation rate of 12.7 microseconds per prediction including the overhead. This is approximately 16.5 million times faster than running `Prospino2`, which took about 3.5 minutes per NLO prediction.

When cross sections are required for a large number of pMSSM points, the leading order (LO) prediction is frequently used as it is faster to compute. However, on average, it is approximately 19% less precise than the prediction at NLO accuracy, while, as noted above, on average the BNN matches the NLO prediction within 3.0% when the few poorly estimated cross section predictions are excluded. Note, however, that even after excluding these outliers, we find that there are still a number of points for which the BNN does worse than the leading order prediction. But, as can be seen in Figure 2, this happens for a small percentage of the pMSSM points we considered.

4.3. The Higgs boson mass function (`OHIGGS`)

The output of the `OHIGGS` data set was analyzed using both regression and classification approaches with the same ensemble of networks. For

both analyses the data set was split into two subsets. One consisted of all pMSSM points where either the true Higgs boson mass was within 2 GeV of 125 GeV [2], or the point's 3 standard deviation interval overlapped with this range. The other subset consisted of all remaining points. Within the first subset, the average percent error was 0.10% and 87.4% of the time the true value was within 3 standard deviations of the predicted value. In the second subset, the percent error was 0.14% and 86.7% of the time the confidence interval contained the true value. If the predictive distributions were Gaussian, these confidence intervals undercover by about 13%, which shows they are not as good as the ones for the cross section data set.

In the classifier approach, the labels were positive if the true Higgs boson mass was within 2 GeV of 125 GeV, and negative if it was not. We claim a prediction to be positive, that is, good, if any part of its confidence interval overlapped the desired range. Using this classification criterion, the precision of the network was 0.926, its recall was 0.997, and its F_1 score was 0.960. We therefore conclude that using the BNN to identify pMSSM parameter points with a low-mass neutral Higgs boson consistent with the measured Higgs boson mass will remove very few pMSSM points that yield Higgs boson masses consistent with observation. Using this approach in conjunction with the regression will also allow very accurate labelling of the selected masses as its error on the selected pMSSM points is low.

We see in Figure 3 that the estimated uncertainty from the ensemble of networks does not match the uncertainty computed from the actual errors. Moreover, in contrast to the results for the cross section, the Higgs boson mass BNN underestimates the uncertainties, though, as expected, the uncertainties are larger where there are fewer data.

4.4. Discussion

The utility of Bayesian neural networks is that they directly approximate the predictive distribution $p(y|x, D)$, that is, they provide a probability density over the space of the quantity being modeled. Moreover, their implementation on GPUs yields a significant increase in prediction speed. In the GPUs we have used (see Appendix), we achieve a computation speed about 50,000 times faster than `SOFTSUSY` and 16.5 million times faster than `Prospino2` running on a single CPU.

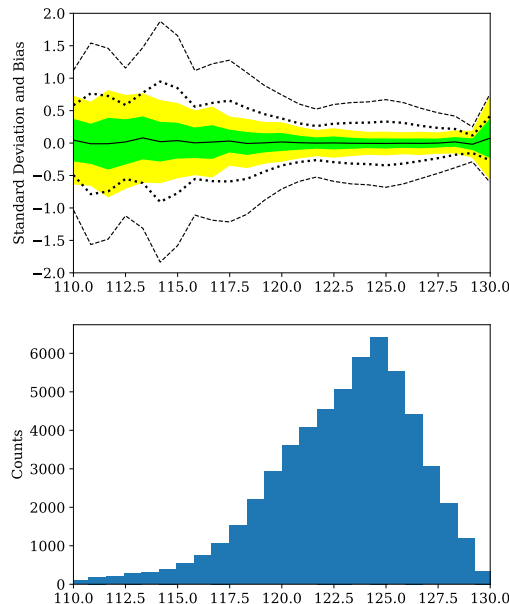


Figure 3: (top) The solid and dotted lines are computed from the errors of the BNN. The black line is the bias of the BNN as a function of the Higgs boson mass. The dotted lines represent the 1 and 2 standard deviation intervals. The green and yellow bands are root mean square intervals computed from the standard deviations furnished by the BNN. (bottom) The distribution of the Higgs boson mass.

In principle, the predictive distribution encodes the uncertainty in a given BNN prediction. There are two kinds of uncertainty that should be accounted for. The first is the uncertainty arising from the fact that a finite amount of data are used to train, that is, fit the models. The second is the uncertainty due to the fact that we do not know which model should be fitted. However, to the degree that the neural network models used in this paper are sufficiently flexible, the uncertainties reported in this paper automatically include both.

However, as is true of all Bayesian inference, the results depend on the likelihood function as well as on the prior. In this work, we have chosen the form of the prior for computational simplicity, with parameters constrained by hyper-priors for added flexibility. However, even granting the form of the hierarchical prior, it is still necessary to choose the values of the hyper-parameters. We have made no attempt, so far, to optimize those choices, which may explain both the over and under estimates of the standard deviations associated with the BNN predictions. But the fact that the problem depends upon hyper-parameters as is true of all machine learning models can be turned into a virtue. For example, by weighting the output of each network in the ensemble of networks by the ratio of the hyper-prior with its hyper-parameters viewed as variables to the hyper-prior with which the HMC sampling was done, we may be able to use standard optimization techniques to improve the results by optimizing the choice of hyper-parameters.

5. Conclusion

Given a large number of predictions of interest from high-dimensional models such as the pMSSM, we showed that BNNs, implemented on GPUs, can successfully model these predictions with computation speeds from 50,000 to 16.5 million times greater than that of the programs that yielded the predictions. This makes it possible to make rapid, accurate, predictions for model points other than those used to construct the BNNs. In particular, we were able to classify accurately whether a given pMSSM parameter point is valid, as determined by **SOFTSUSY**, with a maximum F_1 score of 0.957 and a recall of 0.987. We were also able to predict the cross sections for the production of supersymmetric particles that matched the predictions at NLO accuracy to about 3% on average. Finally, we could classify whether pMSSM parameters would give a

Higgs boson mass of 125 ± 2 GeV with a recall of 0.998 and an F_1 score of 0.942.

These results indicate that it will be possible to more easily filter out pMSSM parameter combinations that are either unphysical or that predict values for the Higgs boson mass inconsistent with observation. It will also be much easier to study the impact of varying different parameters on the production cross sections of supersymmetric particles. Finally, the predictions studied in this paper were just a small number of the potentially interesting ones. Using the methods described in this paper, which are available in the `tensorBNN` [29] package, it should be possible to apply these methods to make rapid predictions of other SUSY observables given a large sample of these predictions from programs such as `SOFTSUSY` and `Prospino2`. Moreover, as noted in our discussion, there is much room for improvement.

6. Acknowledgements

This work was supported in part by the Davidson Research Initiative and the U.S. Department of Energy Award No. DE-SC0010102.

References

- [1] G. Aad, et al., Observation of a new particle in the search for the Standard Model Higgs boson with the ATLAS detector at the LHC, *Phys. Lett. B* 716 (2012) 1–29. [arXiv:1207.7214](https://arxiv.org/abs/1207.7214), doi:10.1016/j.physletb.2012.08.020.
- [2] S. Chatrchyan, et al., Observation of a new boson at a mass of 125 gev with the cms experiment at the lhc, *Physics Letters B* 716 (1) (2012) 30 – 61. doi:<https://doi.org/10.1016/j.physletb.2012.08.021>. URL <http://www.sciencedirect.com/science/article/pii/S0370269312008581>
- [3] C. Quigg, Electroweak symmetry breaking in historical perspective, *Annual Review of Nuclear and Particle Science* 65 (1) (2015) 25–42. [arXiv:https://doi.org/10.1146/annurev-nucl-102313-025537](https://arxiv.org/abs/https://doi.org/10.1146/annurev-nucl-102313-025537), doi:10.1146/annurev-nucl-102313-025537. URL <https://doi.org/10.1146/annurev-nucl-102313-025537>
- [4] S. Dawson, C. Englert, T. Plehn, Higgs physics: It aint over till it is over, *Physics Reports* 816 (2019) 1 – 85, higgs physics: It aint over till it is over. doi:<https://doi.org/10.1016/j.physrep.2019.05.001>. URL <http://www.sciencedirect.com/science/article/pii/S0370157319301784>
- [5] R. Arnowitt, P. Nath, Supersymmetry and supergravity: Phenomenology and grand unification (1993). [arXiv:arXiv:hep-ph/9309277](https://arxiv.org/abs/hep-ph/9309277).
- [6] G. Jungman, M. Kamionkowski, K. Griest, Supersymmetric dark matter, *Physics Reports* 267 (5) (1996) 195 – 373. doi:[https://doi.org/10.1016/0370-1573\(95\)00058-5](https://doi.org/10.1016/0370-1573(95)00058-5). URL <http://www.sciencedirect.com/science/article/pii/0370157395000585>
- [7] A. Djouadi, et al., The Minimal Supersymmetric Standard Model: Group Summary Report. The Minimal supersymmetric standard model: Group summary report, *Tech. Rep. hep-ph/9901246* (1998). URL <http://cds.cern.ch/record/376049>
- [8] M. Cahill-Rowley, J. Hewett, A. Ismail, T. Rizzo, Constraints on higgs properties and susy partners in the pmssm (2013). [arXiv:arXiv:1308.0297](https://arxiv.org/abs/1308.0297).
- [9] T. Severini, *Likelihood Methods in Statistics*, Oxford University Press, 2000.
- [10] W. J. Fawcett, pMSSM studies with ATLAS and CMS, *PoS LHCP2016* (2016) 146. doi:10.22323/1.276.0146.
- [11] G. Aad, et al., Summary of the ATLAS experiments sensitivity to supersymmetry after LHC Run 1 interpreted in the phenomenological MSSM, *JHEP* 10 (2015) 134. [arXiv:1508.06608](https://arxiv.org/abs/1508.06608), doi:10.1007/JHEP10(2015)134.
- [12] V. Khachatryan, et al., Phenomenological MSSM interpretation of CMS searches in pp collisions at $\sqrt{s} = 7$ and 8 TeV, *JHEP* 10 (2016) 129. [arXiv:1606.03577](https://arxiv.org/abs/1606.03577), doi:10.1007/JHEP10(2016)129.
- [13] S. Sekmen, S. Kraml, J. Lykken, F. Moortgat, S. Padhi, L. Pape, M. Pierini, H. B. Prosper, M. Spiropulu, Interpreting LHC SUSY searches in the phenomenological MSSM, *JHEP* 02 (2012) 075. [arXiv:1109.5119](https://arxiv.org/abs/1109.5119), doi:10.1007/JHEP02(2012)075.
- [14] C. F. Berger, J. S. Gainer, J. L. Hewett, T. G. Rizzo, Supersymmetry Without Prejudice, *JHEP* 02 (2009) 023. [arXiv:0812.0980](https://arxiv.org/abs/0812.0980), doi:10.1088/1126-6708/2009/02/023.
- [15] G. Carleo, I. Cirac, K. Cranmer, L. Daudet, M. Schuld, N. Tishby, L. Vogt-Maranto, L. Zdeborov, Machine learning and the physical sciences, *Rev. Mod. Phys.* 91 (4) (2019) 045002. [arXiv:1903.10563](https://arxiv.org/abs/1903.10563), doi:10.1103/RevModPhys.91.045002.
- [16] J. Brehmer, K. Cranmer, G. Louppe, J. Pavez, A guide to constraining effective field theories with machine learning, *Phys. Rev. D* 98 (2018) 052004. doi:10.1103/PhysRevD.98.052004. URL <https://link.aps.org/doi/10.1103/PhysRevD.98.052004>
- [17] S. Caron, J. S. Kim, K. Rolbiecki, R. R. de Austri, B. Stienen, The bsm-ai project: Susy-ai-generalizing lhc limits on supersymmetry with machine learning, *The European Physical Journal C* 77 (4) (2017) 257. doi:10.1140/epjc/s10052-017-4814-9. URL <https://doi.org/10.1140/epjc/s10052-017-4814-9>
- [18] V. M. Abazov, et al., Observation of Single Top Quark Production, *Phys. Rev. Lett.* 103 (2009) 092001. [arXiv:0903.0850](https://arxiv.org/abs/0903.0850), doi:10.1103/PhysRevLett.103.092001.
- [19] T. Aaltonen, et al., First Observation of Electroweak Single Top Quark Production, *Phys. Rev. Lett.* 103 (2009) 092002. [arXiv:0903.0885](https://arxiv.org/abs/0903.0885), doi:10.1103/PhysRevLett.103.092002.
- [20] V. M. Abazov, et al., Evidence for production of single top quarks, *Phys. Rev. D* 78 (2008) 012005. doi:10.1103/PhysRevD.78.012005. URL <https://link.aps.org/doi/10.1103/PhysRevD.78.012005>.

- [21] Y. Xu, Y. X. Meng, W. W. Xu, Applying bayesian neural networks to separate neutrino events from backgrounds in reactor neutrino experiments, *Journal of Instrumentation* 3 (08) (2008) P08005–P08005. doi: <https://doi.org/10.1088/1748-0221/3/08/p08005>.
- [22] P. C. Bhat, Multivariate Analysis Methods in Particle Physics, *Ann. Rev. Nucl. Part. Sci.* 61 (2011) 281–309. doi: [10.1146/annurev.nucl.012809.104427](https://doi.org/10.1146/annurev.nucl.012809.104427).
- [23] J. Brehmer, F. Kling, I. Espejo, K. Cranmer, MadMiner: Machine learning-based inference for particle physics, *Comput. Softw. Big Sci.* 4 (1) (2020) 3. arXiv: [1907.10621](https://arxiv.org/abs/1907.10621), doi: [10.1007/s41781-020-0035-2](https://doi.org/10.1007/s41781-020-0035-2).
- [24] R. M. Neal, Bayesian learning for neural networks, *Lecture Notes in Statistics* doi: [10.1007/978-1-4612-0745-0](https://doi.org/10.1007/978-1-4612-0745-0).
- [25] B. Allanach, Softsusy: A program for calculating supersymmetric spectra, *Computer Physics Communications* 143 (3) (2002) 305 – 331. doi: [https://doi.org/10.1016/S0010-4655\(01\)00460-X](https://doi.org/10.1016/S0010-4655(01)00460-X). URL <http://www.sciencedirect.com/science/article/pii/S001046550100460X>
- [26] W. Beenakker, M. Klasen, M. Krmer, T. Plehn, M. Spira, P. Zerwas, Production of charginos/neutralinos and sleptons at hadron colliders, *Physical Review Letters* 83. doi: [10.1103/PhysRevLett.83.3780](https://doi.org/10.1103/PhysRevLett.83.3780).
- [27] B. Schmidt, The High-Luminosity upgrade of the LHC: Physics and Technology Challenges for the Accelerator and the Experiments, *J. Phys. Conf. Ser.* 706 (2) (2016) 022002. doi: [10.1088/1742-6596/706/2/022002](https://doi.org/10.1088/1742-6596/706/2/022002).
- [28] M. Betancourt, A conceptual introduction to hamiltonian monte carlo, arXiv: Methodology.
- [29] B. Kronheim, M. Kuchera, H. Prosper, TensorBNN: Bayesian inference for neural network training using tensorflow: To be submitted for publication.
- [30] M. Cahill-Rowley, J. L. Hewett, A. Ismail, T. G. Rizzo, Lessons and prospects from the pMSSM after LHC Run I, *Phys. Rev. D91* (5) (2015) 055002. arXiv: [1407.4130](https://arxiv.org/abs/1407.4130), doi: [10.1103/PhysRevD.91.055002](https://doi.org/10.1103/PhysRevD.91.055002).
- [31] C. Goutte, E. Gaussier, A probabilistic interpretation of precision, recall and f-score, with implication for evaluation, in: D. E. Losada, J. M. Fernández-Luna (Eds.), *Advances in Information Retrieval*, Springer Berlin Heidelberg, Berlin, Heidelberg, 2005, pp. 345–359.
- [32] G. Aad, others, T. A. collaboration, Summary of the atlas experiment’s sensitivity to supersymmetry after lhc run 1 —interpreted in the phenomenological mssm, *Journal of High Energy Physics* 2015 (10) (2015) 134. doi: [10.1007/JHEP10\(2015\)134](https://doi.org/10.1007/JHEP10(2015)134). URL [https://doi.org/10.1007/JHEP10\(2015\)134](https://doi.org/10.1007/JHEP10(2015)134)

Appendix A. Training details

A full technical description of the method is given here [29] and we recommend that this reference be consulted in order to provide the relevant context. In this Appendix we describe only those details that are specific to the pMSSM example.

Each data set was trained using the same network design of 5 layers with 50 perceptrons each.

The weights and biases were pre-trained using 3 iteration cycles with 30 epochs each, saving the best network each time as measured by the validation loss. The BNN was initialized with these weights and the activation function, a PReLU, had starting slopes of 0.1. The adaptive step size algorithm was initialized with differing leapfrog step values for the different networks. The starting value is given by the command “leapfrog start”, and the minimum and maximum by “leapfrog min” and “leapfrog max”, respectively (see Table 2). The step sizes also varied during training and are listed in the table as “step size start,” “step size min,” and “step size max.” The initial step size for the hyper-parameters is given by “hyper step size,” but the number of leapfrog steps was always 30. For the regression models, the starting standard deviation for the likelihood function is given by “output σ .” A burn-in period of 100 epochs was used for each network, and the number of epochs each network was trained for can be found under “epochs.” In the adaptive step size algorithm, the grid used always checked 100 different step sizes, and also checked leapfrog steps with an increment given by “leapfrog grid step.” While training, every 10 networks were saved. For reproducibility, all random number generators were seeded. The “PYTHONHASSEED” generator was given the seed 0. We gave `numpy` the seed 42, Python’s random package was assigned 12345, and `TensorFlow` was given the seed 3. The training was done using an Nvidia RTX-2080 TI GPU as well as an Intel Xeon Silver 4210 CPU and the different networks took on the order of two to five days to train.

Parameter	VPAR	XSEC	OHIGGS
leapfrog start	2000	1000	1000
leapfrog min	2000	100	100
leapfrog max	10000	2000	2000
step size start	5e-5	1e-5	5e-5
step size min	2.5e-5	5e-6	2.5e-5
step size max	2e-4	2e-5	1e-4
leapfrog grid step	10	1	1
hyper step size	5e-6	1e-5	1e-5
output σ	-	0.1	0.5
epochs	1750	13500	2850

Table A.3: `tensorBNN` network training parameters.